

Absolute Structures of a Mirror Pair of Infinite $\text{Na}(\text{H}_2\text{O})_4^+$ -Connected ε -Keggin– Al_{13} Species

Hui Wang, Jin-Liang Gu, Yu-Wei Guo, Yu Ma, Ning-Ning Yu, and Zhong Sun*

Cite This: *ACS Omega* 2024, 9, 20185–20195

Read Online

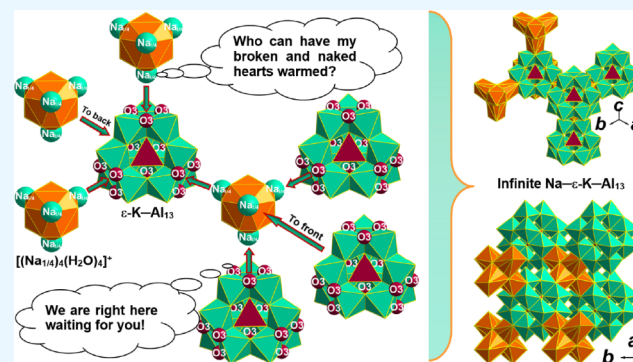
ACCESS |

Metrics & More

Article Recommendations

Supporting Information

ABSTRACT: The absolute structures of a pair of infinite $\text{Na}(\text{H}_2\text{O})_4^+$ -connected ε -Keggin– Al_{13} species ($\text{Na}-\varepsilon\text{-K}-\text{Al}_{13}$) that were inversion structures and mirror images of each other were determined. Single crystals obtained by adding A_2SO_4 ($\text{A} = \text{Li}, \text{Na}, \text{K}, \text{Rb},$ or Cs) solution to NaOH -hydrolyzed AlCl_3 solution were subjected to X-ray structure analyses. The statistical results for 36 single crystals showed that all the crystals had almost the same unit cell parameter, belonged to the same $F43m$ space group, and possessed the same structural formula $[\text{Na}(\text{H}_2\text{O})_4\text{AlO}_4\text{Al}_{12}(\text{OH})_{24}(\text{H}_2\text{O})_{12}](\text{SO}_4)_4 \cdot 10\text{H}_2\text{O}$. However, the crystals had two inverse absolute structures (denoted A and B), which had a crystallization ratio of 1:1. From Li^+ to Cs^+ , with increasing volume of the cation coexisting in the mother solution, the degree of disorder of the four H_2O molecules in the $\text{Na}(\text{H}_2\text{O})_4^+$ hydrated ion continuously decreased; they became ordered when the cation was Cs^+ . Absolute structures A and B are the first two infinite aluminum polycations connected by statistically occupied $[(\text{Na}_{1/4})_4(\text{H}_2\text{O})_4]^+$ hydrated ions. The three-dimensional structure of the infinite $\text{Na}-\varepsilon\text{-K}-\text{Al}_{13}$ species can be regarded as the assembly of finite $\varepsilon\text{-K}-\text{Al}_{13}$ species linked by $[(\text{Na}_{1/4})_4(\text{H}_2\text{O})_4]^+$ in a 1:1 ratio. In this assembly, each $[(\text{Na}_{1/4})_4(\text{H}_2\text{O})_4]^+$ is connected to four $\varepsilon\text{-K}-\text{Al}_{13}$ and each $\varepsilon\text{-K}-\text{Al}_{13}$ is also connected to four $[(\text{Na}_{1/4})_4(\text{H}_2\text{O})_4]^+$ in tetrahedral orientations to form a continuous rigid framework structure, which has an inverse spatial orientation between absolute structure A and B. This discovery clarifies that the $\varepsilon\text{-K}-\text{Al}_{13}$ (or $\varepsilon\text{-K}-\text{GaAl}_{12}$) species in $\text{Na}[\text{MO}_4\text{Al}_{12}(\text{OH})_{24}(\text{H}_2\text{O})_{12}](\text{XO}_4)_4 \cdot n\text{H}_2\text{O}$ ($\text{M} = \text{Al}, \text{Ga}; \text{X} = \text{S}, \text{Se}; n = 10-20$) exists as discrete groups and deepens understanding of the formation and evolution process of polyaluminum species in forcibly hydrolyzed aluminum salt solution. The reason why Na^+ statistically occupies the four sites was examined, and a formation and evolution mechanism of the infinite $\text{Na}-\varepsilon\text{-K}-\text{Al}_{13}$ species was proposed.



1. INTRODUCTION

The types and quantities, concentrations and distributions, and formation and evolution rules of polymeric aluminum species in hydrolyzed aluminum (Al) solution are important scientific problems for revealing the action mechanisms of Al-series flocculants, synthesizing highly efficient coagulants, understanding the transportation and transformation laws of Al in the global environment, and preventing Al pollution.^{1–4} However, these problems have perplexed scientists for almost a century. Because various species coexist in a hydrolyzed Al solution, the distribution of each component is influenced by any change in synthesis conditions, such as basification degree ($B = [\text{OH}]/[\text{Al}]$), temperature, pressure, Al concentration, type and strength of basification agents, and the presence of anions. It is difficult to isolate pure polyaluminum compounds from solution and even more difficult to grow a large enough single crystal for structure analysis. Even so, single-crystal X-ray diffraction (XRD) is still the best way to obtain the exact structure of a material compared with other investigation methods such as Al-ferron complexation-timed spectrophotometry,⁵ ^{27}Al nuclear magnetic resonance spectroscopy,^{6,7} and

mass spectrometry.^{8,9} This is because XRD might give some information about the polynuclear complexes that seem to exist in hydrolyzed Al salt solutions.^{10,11} The number of Al species with known structures is limited (Figure S1).^{12–40} How an Al monomer develops into aluminum hydroxide ($\text{Al}(\text{OH})_3$) is still debated, and the hydrolytic chemistry of Al salt solutions remains poorly understood.^{1,2} Therefore, each discovery of a new Al-based structure has far-reaching influences on fields such as geochemistry, environmental science, biochemistry, medicine, and water pollution control chemistry.^{1–4,41–44} In particular, the $\varepsilon\text{-K}-\text{Al}_{13}$ polycation (K is the Keggin structure, $[\text{AlO}_4\text{Al}_{12}(\text{OH})_{24}(\text{H}_2\text{O})_{12}]^{7+}$) laid the foundation for the “cage-like” K– Al_{13} aggregation model^{12–15} and has been

Received: January 14, 2024

Revised: April 7, 2024

Accepted: April 12, 2024

Published: April 25, 2024

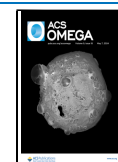


Table 1. Crystallographic Data and Structure Refinement Parameters for Absolute Structures A and B

	isolated by adding Cs ₂ SO ₄ , OS atom ordered		isolated by adding K ₂ SO ₄ , OS atom disordered	
	absolute structure A	absolute structure B	absolute structure A	absolute structure B
temperature	296 K	296 K	100 K	100 K
empirical formula	Al ₁₃ H ₇₆ NaO ₇₀ S ₄	Al ₁₃ H ₇₆ NaO ₇₀ S ₄	Al ₁₃ H ₇₆ NaO ₇₀ S ₄	Al ₁₃ H ₇₆ NaO ₇₀ S ₄
formula weight	1698.57	1698.57	1698.57	1698.57
crystal system	cubic	cubic	cubic	cubic
space group	$F\bar{4}3m$ (No. 216)	$F\bar{4}3m$ (No. 216)	$F\bar{4}3m$ (No. 216)	$F\bar{4}3m$ (No. 216)
<i>a</i> (Å)	17.8218(14)	17.834(3)	17.7728(15)	17.7792(16)
volume (Å ³)	5660.5(13)	5672(3)	5613.9(14)	5620.0(15)
<i>Z</i>	4	4	4	4
<i>D_m</i> (g/cm ³)	1.974	1.974		
<i>D_c</i> (g/cm ³)	1.993	1.989	2.010	2.008
<i>F</i> (000)	3520	3520	3520	3520
crystal size (mm ³)	0.31 × 0.31 × 0.31	0.37 × 0.37 × 0.37	0.32 × 0.32 × 0.32	0.31 × 0.31 × 0.31
crystal shape	tetrahedron	tetrahedron	tetrahedron	tetrahedron
color	colorless	colorless	colorless	colorless
λ (Mo <i>K</i> α) (Å)	0.71073	0.71073	0.71073	0.71073
absorption coefficient (mm ⁻¹)	0.533	0.532	0.537	0.537
θ range (degree)	4.99–28.46	4.98–28.43	5.00–28.98	5.00–28.99
limiting indices	–12 ≤ <i>h</i> ≤ +23 –10 ≤ <i>k</i> ≤ +23 –23 ≤ <i>l</i> ≤ +4	–19 ≤ <i>h</i> ≤ +12 –23 ≤ <i>k</i> ≤ +3 –16 ≤ <i>l</i> ≤ +23	–1 ≤ <i>h</i> ≤ +24 –18 ≤ <i>k</i> ≤ +11 –17 ≤ <i>l</i> ≤ +23	–10 ≤ <i>h</i> ≤ +19 –12 ≤ <i>k</i> ≤ +24 –24 ≤ <i>l</i> ≤ +7
all reflections/completeness (%)	3356/98.3	3134/98.6	3476/98.6	3471/98.6
<i>R_{int}</i> (%) / <i>R_σ</i> (%)	2.15/1.94	1.80/1.53	2.07/1.99	2.22/2.17
data/restraints/parameters	745/18/67	721/18/67	791/17/74	759/17/74
observed reflections [<i>I</i> > 2σ(<i>I</i>)]	715	695	777	749
GOF on <i>F</i> ² [<i>I</i> > 2σ(<i>I</i>)]	1.152	1.124	1.095	1.106
GOF on <i>F</i> ² (all data)	1.174	1.143	1.127	1.139
<i>R</i> ₁ (%) / <i>wR</i> ₂ (%) [<i>I</i> > 2σ(<i>I</i>)]	3.47/10.58	3.43/10.18	3.47/8.45	3.57/8.62
<i>R</i> ₁ (%) / <i>wR</i> ₂ (%) (all data)	3.72/10.93	3.59/10.51	3.55/8.52	3.62/8.66
largest difference peak/hole (e/Å ³)	0.666/–0.300	0.704/–0.339	0.464/–0.387	0.509/–0.418
residual electron density (e/Å ³)	0.070	0.072	0.062	0.065
Flack factor for absolute structure	0.02(7)	0.07(6)	0.02(4)	0.08(4)

widely studied. For example, Furrer *et al.*⁴⁵ showed that the flocs in polluted streams originated from the aggregation of ϵ -K–Al₁₃ species. Phillips and coworkers found that the ¹⁷OH₂ exchange rates of OH ligands were extremely sensitive to subtle differences in the local structure and Brønsted acidity of the surface.⁴⁶ Rustad *et al.*⁴⁷ reported the mechanistic pathways of ϵ -K–Al₁₃ species and ascribed the sensitivity of their exchange rates to single-atom substitutions. Hunter and Ross found that ϵ -K–Al₁₃ was more toxic than the monomer in forested spodosol soils.⁴⁸ Pinnavaia reported that ϵ -K–Al₁₃-pillared montmorillonites can be used as a petroleum cracking catalyst and large molecule adsorbent.⁴⁹

The structures of ϵ -K–Al₁₃ species were first solved in 1960–1963 by Johansson's group.^{12–15} They solved the structures of cubic Na₂O·13Al₂O₃·8XO₃·*y*H₂O (*X* = S, Se; *y* = 68–76) and monoclinic 13Al₂O₃·6SO₃·*z*H₂O (*z* = ~ 79). The structure of the cubic selenate was solved from rotation and Weissenberg photographs. Because the Na atoms could not be located from the difference maps, however, chemical analysis confirmed that about four Na atoms were present in the unit cell, so the structural formula was assigned as Na[Al₁₃O₄(OH)₂₄(H₂O)₁₂](SeO₄)₄·12.5H₂O.¹⁴ The structure of the cubic sulfate was solved in 1997 by Parker *et al.*;¹⁶ they found the positions of Na⁺ but did not identify their H₂O ligands, so the structural formula was then given as Na[Al₁₃O₄(OH)₂₄(H₂O)₁₂](SO₄)₄·10H₂O. The structure of the monoclinic sulfate was solved in 1963 by Johansson, who

reported a structural formula of [Al₁₃O₄(OH)₂₅(H₂O)₁₁](SO₄)₃·16H₂O and suggested that the structure of each complex ion was similar to that in the cubic selenate with only one proton less than the number in ϵ -K–Al₁₃.¹⁵ An *et al.*⁵⁰ found that the tetrahedral (*T_d*) crystals of the cubic sulfate can be transformed into plate-like monoclinic sulfate ones by soaking in water.

Our research group obtained two kinds of cubic sulfate by adding A₂SO₄ (*A* = Li, Na, K, Rb, and Cs) solutions to NaOH-hydrolyzed AlCl₃ solutions. All of the samples crystallized as *T_d* single crystals. However, the structure analysis and conformation statistics results of 36 single crystals from the five reaction mixtures indicated that the ϵ -K–Al₁₃ groups in the two sulfates were not only connected together by [(Na_{1/4})₄(H₂O)₄]⁺ to form continuous infinite three-dimensional (3D) framework structures but also had inverse orientations. Correspondingly, the distributions of SO₄²⁻ and the interstitial H₂O molecules in a respective unit cell were also inverted, so two different absolute structures (A and B) formed, where one was the inversion structure of the other. The ratio of absolute structures A and B in each reaction mixture was 1:1. Also, it was found that the four H₂O molecules in [(Na_{1/4})₄(H₂O)₄]⁺ were ordered in the case of Cs⁺ (the largest cation used) and disordered for smaller Li⁺, Na⁺, K⁺, and Rb⁺. In this paper, the single crystals isolated by adding Cs₂SO₄ and K₂SO₄ are selected as representatives in which the four H₂O molecules in [(Na_{1/4})₄(H₂O)₄]⁺ are

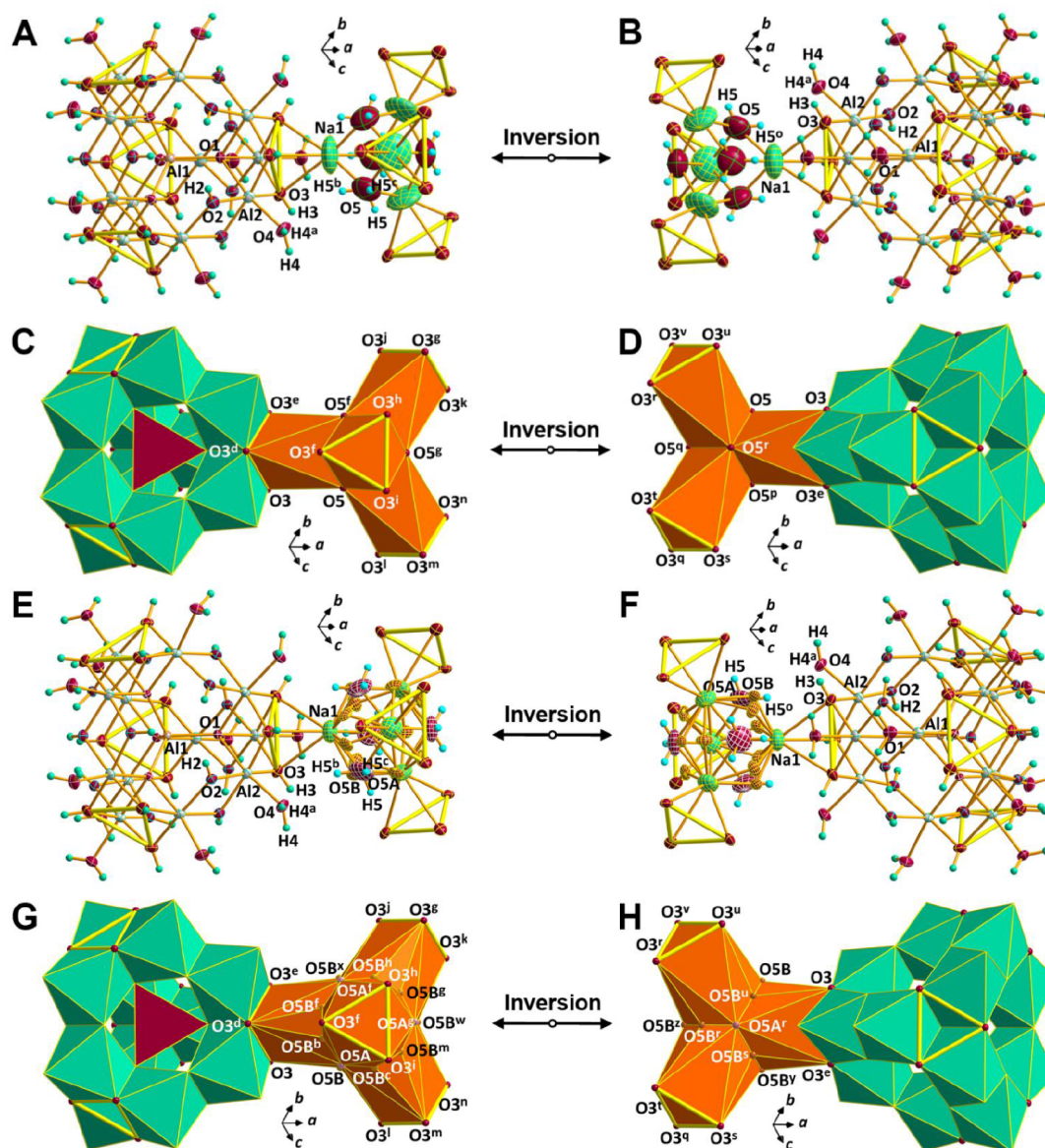


Figure 1. Structures of $[\text{Na}(\text{H}_2\text{O})_4\text{AlO}_4\text{Al}_{12}(\text{OH})_{24}(\text{H}_2\text{O})_{12}]^{8+}$ ($\text{Na}-\epsilon\text{-K}-\text{Al}_{13}$) species in absolute structures A and B isolated by adding Cs_2SO_4 and K_2SO_4 to NaOH -hydrolyzed AlCl_3 solution. The yellow bold-edged triangles represent the joint faces between the statistically occupied $\text{Na}(\text{H}_2\text{O})_4^+$ and $\epsilon\text{-K}-\text{Al}_{13}$ groups in infinite structures. (A and B) Ellipsoid-stick representations with a probability of 50% (site occupancies: Na1, 1/4; H5, 2/3; others, 1). (C and D) Polyhedral representations that show the connection relationships between the statistically occupied $\text{Na}(\text{H}_2\text{O})_4^+$ and $\epsilon\text{-K}-\text{Al}_{13}$ groups. O5 atoms are not disordered when Cs_2SO_4 was added. (E, F) Ellipsoid-stick representations with a probability of 50% (site occupancies: Na1, 1/4; O5A, 0.55; O5B, 0.15; H5, 2/3; others, 1). (G and H) Polyhedral representations that show the connection relationships between the statistically occupied $\text{Na}(\text{H}_2\text{O})_4^+$ and $\epsilon\text{-K}-\text{Al}_{13}$ groups. Each O5 atom was disordered as an O5A and three O5B when K_2SO_4 was added. (A and C) The structure of $\text{Na}-\epsilon\text{-K}-\text{Al}_{13}$ in absolute structure A and (B and D) the structure of $\text{Na}-\epsilon\text{-K}-\text{Al}_{13}$ in absolute structure B crystallized by adding Cs_2SO_4 . Diffraction measurements were conducted at 296 K. (E and G) The structure of $\text{Na}-\epsilon\text{-K}-\text{Al}_{13}$ in absolute structure A and (F and H) the structure of $\text{Na}-\epsilon\text{-K}-\text{Al}_{13}$ in absolute structure B crystallized by adding K_2SO_4 . Diffraction measurements were conducted at 100 K. Symmetry transformations used to generate equivalent atoms were, a: y, x, z ; b: $y, 1/2-z, 1/2-x$; c: $1/2-z, x, 1/2-y$; d: y, z, x ; e: z, x, y ; f: $y, 1/2-x, 1/2-z$; g: $1/2-x, 1/2-y, z$; h: $x, 1/2-y, 1/2-z$; i: $z, 1/2-x, 1/2-y$; j: $1/2-x, 1/2-z, y$; k: $1/2-y, 1/2-z, x$; l: $1/2-x, y, 1/2-z$; m: $1/2-x, z, 1/2-y$; n: $1/2-y, x, 1/2-z$; o: $y, -1/2-z, -1/2-x$; p: $y, -1/2-x, -1/2-z$; q: $-1/2-x, -1/2-y, z$; r: $-1/2-y, x, -1/2-z$; s: $-1/2-x, -1/2-z, y$; t: $-1/2-y, -1/2-z, x$; u: $-1/2-x, y, -1/2-z$; v: $-1/2-x, z, -1/2-y$; w: $1/2-y, z, 1/2-x$; x: $1/2-z, 1/2-x, y$; y: $-1/2-z, -1/2-x, y$; z: $-1/2-y, z, -1/2-x$.

ordered and disordered, respectively. The absolute structures of these crystals are determined and discussed in detail.

2. EXPERIMENTAL DETAILS

2.1. Synthesis. Aqueous NaOH solution (0.25 mol/L, 240 mL) was added dropwise to a rapidly stirred AlCl_3 solution (0.25 mol/L, 100 mL) at 80 °C. After aging at 80 °C for 24 h,

the solution was filtered through a filter membrane (0.45 μm) and then cooled to room temperature to form a stock solution with $B = 2.4$ and $\text{pH} = 4.26$. Aqueous Li_2SO_4 , Na_2SO_4 , K_2SO_4 , Rb_2SO_4 , and Cs_2SO_4 solutions (0.25 mol/L, 4 mL) were poured into five aliquots of the stock solution (10 mL). After 3 weeks, colorless T_d single crystals were obtained from the

mixtures with Li^+ , Na^+ , K^+ , Rb^+ , and Cs^+ in yields of 40.6%, 39.5%, 41.5%, 41.7%, and 41.9%, respectively.

2.2. Single-Crystal X-ray Structure Analysis. First, one T_d single crystal isolated from each mixture was selected for structure analysis at room temperature. Diffraction intensities were recorded on a Bruker SMART X-ray diffractometer (graphite monochromator and charge-coupled device area detector), multiscan absorption corrections were applied using SADABS,⁵¹ and the diffraction data were reduced using Bruker SAINT.⁵² Initial structures were solved by direct methods using SHELXT-2014,⁵³ and the coordinates of the rest of the non-H atoms were obtained from difference Fourier maps. All coordinates and anisotropic thermal parameters of the non-H atoms were refined by full-matrix least-squares techniques based on F^2 using SHELXL-2017.⁵⁴ All coordinates of H atoms were also obtained from difference Fourier maps, and their positions and isotropic thermal parameters were constrained. It was found that the five crystals had two kinds of absolute structures, A and B. To investigate the percentages of absolute structures A and B in each reaction mixture, four or eight single crystals in the same mixture were randomly chosen for X-ray structure analysis. Statistical analysis of a total of 36 single crystals showed that the ratio of A to B in each mixture was 1:1, as listed in Table S3. To determine whether the four coordinated H_2O molecules in $[(\text{Na}_{1/4})_4(\text{H}_2\text{O})_4]^+$ needed to be treated as disordered, the site occupancies of O5A atoms in 16e and O5B atoms in 48h Wyckoff positions were also refined. To obtain the accurate coordinates of all H atoms from the difference Fourier maps, diffraction intensity data were also collected at low temperature (100 K) and the resolution ratios were extended to 0.60 Å. Resolution ratios were limited to 0.75 Å in final refinements to compare the refinement results to literature values.

2.3. Density Measurement. The densities of the five samples were measured by the kerosene pycnometer method at 23.0 °C; the measured and calculated results are listed in Table S2. The measurement process is described in the Supporting Information. From Table S2, it is clear that the average measured density of 1.98 is close to the average calculated density of 1.99 obtained from the X-ray single-crystal structure analysis at 23.0 °C and the measured density of 1.97 reported by Johansson and colleagues.¹²

2.4. XRD Characterization. The XRD patterns of the five samples were recorded on a PANalytical Empyrean powder X-ray diffractometer with Cu $K\alpha$ radiation ($\lambda = 1.5418$ Å) operating at 40 kV and 40 mA. The obtained patterns matched those reported in PDF 49-457 and agreed well with the simulated patterns calculated from structural parameters (Figure S5). The crystallographic data and structure refinement parameters of the crystals are listed in Table 1.

2.5. Further Characterization. The results of thermogravimetric (TG), infrared (IR), and X-ray fluorescence (XRF) analyses are provided in the Supporting Information.

3. RESULTS AND DISCUSSION

Figures 1 and 2 reveal that the giant polycations in absolute structures A and B are all composed of numerous statistically occupied $[(\text{Na}_{1/4})_4(\text{H}_2\text{O})_4]^+$ and $\epsilon\text{-K-Al}_{13}$ groups. Each $[(\text{Na}_{1/4})_4(\text{H}_2\text{O})_4]^+$ is connected to four $\epsilon\text{-K-Al}_{13}$ and each $\epsilon\text{-K-Al}_{13}$ is also connected to four $[(\text{Na}_{1/4})_4(\text{H}_2\text{O})_4]^+$ by sharing the 12 O3 atoms located on the four triangular surfaces of each corner-cut tetrahedral $\epsilon\text{-K-Al}_{13}$ (yellow triangles with bold edges in Figure 1), forming 3D infinite framework

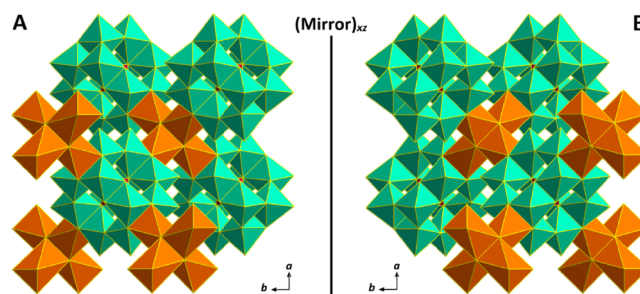


Figure 2. Connection relationships between $\text{Na}(\text{H}_2\text{O})_4^+$ and $\epsilon\text{-K-Al}_{13}$ groups in infinite $\text{Na-}\epsilon\text{-K-Al}_{13}$ species and their spatial orientations in absolute structures A and B isolated by adding Cs_2SO_4 to NaOH -hydrolyzed AlCl_3 solution. In these structures, the coordinated water molecules of the statistically occupied Na^+ sites are not disordered. All structural parameters were determined from diffraction data collected at 296 K, showing a mirror-image relationship relative to the xz plane viewed along the c axis. Similar connection relationships obtained when K_2SO_4 was added to a NaOH -hydrolyzed AlCl_3 solution can be found in Figure S2B.

structures. The spatial orientations of A and B are different, and they are inversion structures of each other (also see Figure S2B). Thus, $\text{Na}(\text{H}_2\text{O})_4^+$ -connected $\epsilon\text{-K-Al}_{13}$ forms the basic repeating unit. The structural formulas of the infinite polycations in absolute structures A and B can all be written as $[\text{Na}(\text{H}_2\text{O})_4\text{AlO}_4\text{Al}_{12}(\text{OH})_{24}(\text{H}_2\text{O})_{12}]^{8+}$, which we hereafter refer to as $\text{Na-}\epsilon\text{-K-Al}_{13}$.

The structure of $\text{Na}(\text{H}_2\text{O})_4^+$ is not as imagined with Na^+ at the center of a tetrahedron formed by the four O atoms of the four coordinated H_2O molecules. Instead, Na^+ statistically appears on the outside of the four triangular planes of the tetrahedron with a site occupancy (SO) of 1/4 (the reason for this will be discussed later). The crystals obtained by adding A_2SO_4 ($\text{A} = \text{Li}, \text{Na}, \text{K}, \text{Rb}, \text{and Cs}$) show a structural difference related to the disorder of the four O atoms. With increasing cation volume, the degree of disorder of the four O atoms (labeled as O5) continuously decreases. When the cation is Cs^+ , the O5 atoms become ordered (see Figure S3). In the cases of other cations, each O atom is disordered with three O5B surrounding each O5A. Because each of the four O5 (or O5A) atoms is located on a 3 (rotation axis), the two H atoms connected to it occupy three equivalent sites (SO = 2/3). Therefore, $[(\text{Na}_{1/4})_4(\text{H}_2\text{O})_4]^+$ resembles an Na-capped tetrahedron (Figure 6) with ideal T_d symmetry before it is connected to the four $\epsilon\text{-K-Al}_{13}$ groups.

The $\epsilon\text{-K-Al}_{13}$ groups in absolute structures A and B were all composed of an AlO_4 tetrahedron and 12 AlO_6 octahedra. The AlO_4 core was connected to four Al_3O_{13} triads (three AlO_6 linked together by vertex- and edge-sharing) by sharing its four vertices, and the four triads connect to each other by edge-sharing to form a shell. If the 12 O4 atoms (representing the 12 coordinated H_2O molecules) were linked by lines, the outline of the core-shell-structured $\epsilon\text{-K-Al}_{13}$ group can be visualized as a corner-cut tetrahedron with ideal T_d symmetry, as shown in Figure S2A.

When the O5 atom is not disordered, the structure with Na-O bonds is simple. Each of the four statistically 1/4-occupied Na^+ forms six chemical bonds (selected bond lengths and angles of absolute structures A and B are listed in Table S10). Of these six bonds, three identical Na-O bond lengths (2.02 Å) that are 0.25 Å shorter than the sum of the covalent radii⁵⁵ of Na (1.54 Å) and O (0.73 Å) atoms, and three

identical Na–O3 bond lengths (2.50 Å) that are 0.08 Å longer than the sum of the effective ionic radii⁵⁶ of Na⁺ (1.02 Å) and O²⁻ (1.40 Å), giving an average bond length of 2.26 Å. When the O5 atom is disordered, each of the four Na⁺ statistically participates in forming 12 chemical bonds: three identical Na–OSA bond lengths (2.12 Å) that are 0.15 Å shorter than the sum of covalent radii of Na and O atoms, six identical Na–OSB bond lengths (1.78 Å) that are 0.49 Å shorter than the sum of covalent radii, and three identical Na–O3 bonds with a length of 2.54 Å, which is 0.12 Å longer than the sum of effective ionic radii of Na⁺ and O²⁻. The weighted average bond length in this case is 2.29 Å:

$$\frac{0.55 \times 2.12 \times 3 + 0.15 \times 1.78 \times 6 + 1 \times 2.54 \times 3}{0.55 \times 3 + 0.15 \times 6 + 1 \times 3} = 2.29$$

Therefore, the average Na–O bond length when the O5 atom is ordered or disordered (2.26 or 2.29 Å, respectively) is similar to the sum of covalent radii (2.27 Å) and 0.12–0.15 Å shorter than the average bond length in discrete Na– δ -K–Al₁₃ reported by Rowsell and Nazar (2.41 Å),¹⁸ indicating that Na(H₂O)₄⁺ and ϵ -K–Al₁₃ are tightly connected together by strong chemical bonds. In other words, the 3D framework structures of the infinite Na– ϵ -K–Al₁₃ species in absolute structure A and B are rigid, as shown in Figures 3 and S2C.

The orientation, distribution, and interrelation of the Na– ϵ -K–Al₁₃ polycations, SO₄²⁻, and interstitial H₂O molecules in a unit cell in absolute structures A and B can be understood as

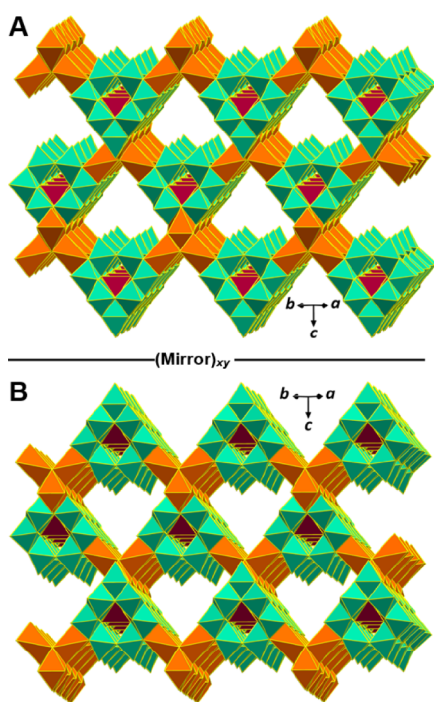


Figure 3. Rigid framework structures of infinite Na– ϵ -K–Al₁₃ species in absolute structures A and B isolated by adding Cs₂SO₄ to NaOH-hydrolyzed AlCl₃ solution, in which the coordinated water molecules associated with the statistically occupied Na⁺ are not disordered. All structural parameters were determined from diffraction data collected at 296 K, showing a mirror–image relationship relative to the *xy* plane when viewed along a direction close to [110]. Similar structures obtained when K₂SO₄ was added to NaOH-hydrolyzed AlCl₃ solution can be found in Figure S2C.

the cubic closest packing (ccp) of spheres of unequal diameter, similar to the case of cubic ZnS. It is clear from Figure 4 that

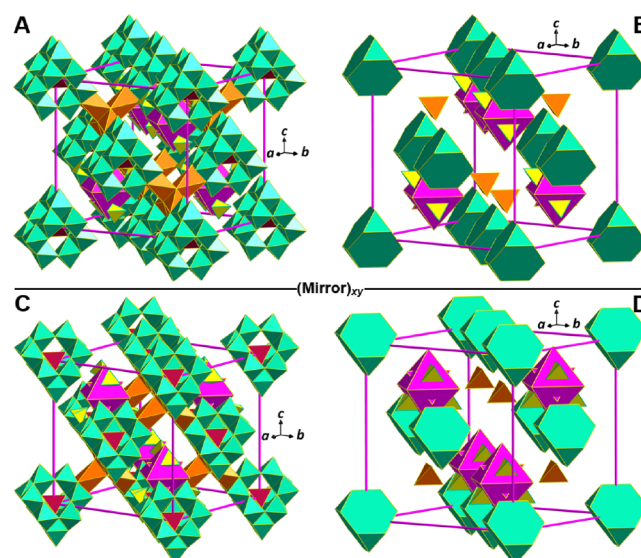


Figure 4. Crystal structures of [Na(H₂O)₄AlO₄Al₁₂(OH)₂₄(H₂O)₁₂](SO₄)₄·10H₂O in absolute structures A (top) and B (bottom). (A and C) Distributions of the four molecules in respective unit cells (color code: orange, Na(H₂O)₄; amaranthine, AlO₄; cyan, AlO₆; yellow, SO₄; pink, O₄ tetrahedra and O₆ octahedra represent interstitial H₂O molecules). (B and D) Simplified polyhedral representations of the molecular distributions in respective unit cells, in which only the 13 Al nuclei of each ϵ -K–Al₁₃ group, the four statistically 1/4-occupied Na nuclei of each Na(H₂O)₄⁺, the four S nuclei of each four SO₄²⁻, and the ten O nuclei of each ten interstitial H₂O molecules are shown as different polyhedra for clarity [color code: cyan corner-cut tetrahedra, Al₁₃; orange tetrahedra, (Na_{1/4})₄; yellow tetrahedra, S₄; pink tetrahedra and octahedra, O₄ and O₆, respectively].

there are four [Na(H₂O)₄AlO₄Al₁₂(OH)₂₄(H₂O)₁₂](SO₄)₄·10H₂O molecules in a unit cell, and the four molecules can be separated into three groups: the first includes four ϵ -K–Al₁₃ groups ([AlO₄Al₁₂(OH)₂₄(H₂O)₁₂]⁷⁺, corner-cut tetrahedron), the second includes four Na(H₂O)₄⁺ (actually, the Na(H₂O)₄⁺ and ϵ -K–Al₁₃ groups connect with each other tightly to form the Na– ϵ -K–Al₁₃ species; they were separated here just to help explain their distributions), and the third includes 16 SO₄²⁻ and 40 interstitial H₂O molecules. The third group can be further separated into four small groups, each of which consists of four SO₄²⁻ and ten interstitial H₂O molecules (hereafter, this group is abbreviated as 4S10W). The interrelation between the members within 4S10W is shown on the right in Figure S2A. Six (O7) of the ten interstitial H₂O molecules form an octahedron, the remaining four (O6) are symmetrically located at the outsides of the four triangular planes of the octahedron, and the four SO₄²⁻ are symmetrically positioned at the outsides of the other four triangular planes of the octahedron with one corner of each SO₄ tetrahedron facing toward the center of the triangular plane.

The left of Figure S2A reveals that each corner-cut tetrahedron has four equilateral triangles and four inequilateral hexagons on its surface. The distribution of the ϵ -K–Al₁₃ groups in a unit cell can be regarded as the result of ccp of the corner-cut tetrahedra; their centers (Al1 atoms) are located on the vertices and face-centered positions of the unit cell; i.e., the Wyckoff 4*a* sites and their coordinates are 0,0,0; 1/2,1/2,0; 1/

2,0,1/2; and 0,1/2,1/2. Also, as a result of the ccp, eight tetrahedral voids are formed, each of which is formed from four corner-cut tetrahedra (one located on the vertex and the other three located on the face-centered positions closest to the vertex). The void centers are located on the four body diagonals of a unit cell, i.e., the Wyckoff 4c and 4d sites. The void coordinates at 4c sites are 1/4,1/4,1/4; 3/4,3/4,1/4; 3/4,1/4,3/4; and 1/4,3/4,3/4 and those at 4d sites are 3/4,1/4,1/4; 1/4,3/4,1/4; 1/4,1/4,3/4; and 3/4,3/4,3/4. The distances from each center to the closest vertex and three face-centered positions are all $\sqrt{3}a/4$, where a is the unit cell parameter. The volume and shape of the eight tetrahedral voids would be the same if the objects in the ccp arrangement were spheres with an equal diameter. However, here the ccp objects are corner-cut tetrahedra, and the vertical distance from the center of each tetrahedron (Al1 atom) to its four triangular surfaces (3.864 Å) is about 1 Å longer than to its four hexagonal surfaces (2.810 Å) in crystals isolated by adding Cs_2SO_4 , as determined by Diamond software.⁵⁷ Therefore, the eight tetrahedral voids fall into two groups based on their volume and shape. Each of the four voids in the small-volume group is constructed from four equilateral triangular surfaces provided by four corner-cut tetrahedra forming a small cubic octahedral void, i.e., a corner-cut cube (four corners were cut more, and the other four were cut less in respective tetrahedral orientations). The eight sections of each of these voids are all triangles but four are larger and the other four smaller, as shown in Figure 5A. The volume of these smaller voids of 226 Å³ was calculated as the volume of the cube minus the total volume of the eight cut-away triangular pyramids. Each of the four voids in the large-volume group was generated from four inequilateral hexagonal surfaces provided by four corner-cut tetrahedra to form a cubic octahedral void, i.e., another kind of corner-cut cube (four corners were cut much more, and the other four were cut a little less in respective tetrahedral orientations). The eight sections of the larger voids are all hexagons but four are larger and the other four smaller, as shown in Figure 5B. The volume of 805 Å³ for these voids was calculated as the volume of the cube minus the total volume of the eight cut-away inequilateral hexagonal pyramids and 12 inequilateral tetrahedra under the 12 edges of the cube. It is obvious that each small void is occupied by a $\text{Na}(\text{H}_2\text{O})_4^+$ that is connected to 12 OH ligands (O3) that come from four $\epsilon\text{-K-Al}_{13}$ groups. The small voids are positioned slightly lower than the edge-centered positions of the four triangular surfaces. Each larger void is occupied by a 4S10W unit, which forms a hydrogen-bonded system (that will be discussed later) with H_2O and OH ligands that come from four $\epsilon\text{-K-Al}_{13}$ groups. Each larger void is located on or a little lower than the middle area of the four hexagonal surfaces, as shown in Figure 5C. Thus, each corner-cut tetrahedron connects to four small voids by sharing its four triangular surfaces (forming rigid chemical bonds with the $\text{Na}(\text{H}_2\text{O})_4^+$ in the void) and also contacts with four large voids by sharing its four hexagonal surfaces (forming flexible hydrogen bonds with the 4S10W unit occupying the void), as shown in Figure 5D.

The distributions and lengths of hydrogen bonds in absolute structures A and B are shown in Figure S4 and Tables S1 and S1'. The lengths of corresponding hydrogen bonds in A and B are almost the same, so average values have been used below. The interrelation between the 4S10W units within a small group was maintained by forming thirty-six weak hydrogen bonds, including 12 O6–H6...O8 (2.25 Å), 12 O7–H7...O8

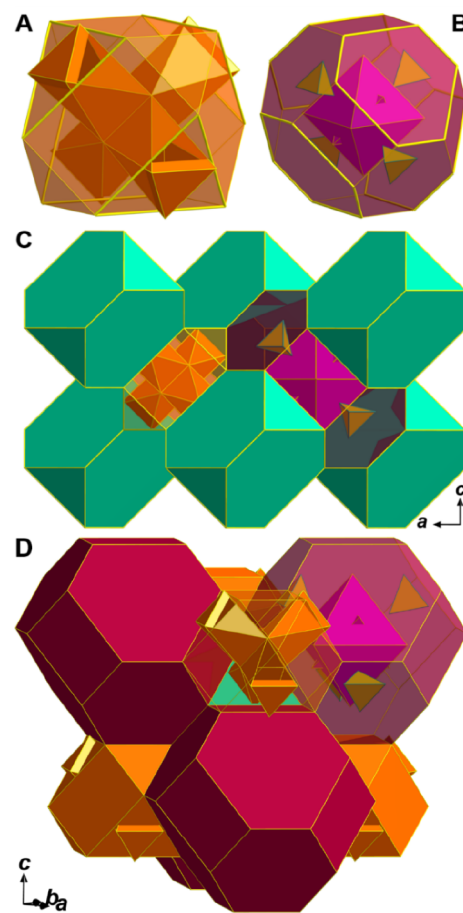


Figure 5. Two kinds of cubic octahedral voids and their interrelation with the corner-cut tetrahedra. (A) The small void (here, it was enlarged for clarity) is constructed from four equilateral triangles (thick yellow lines) that come from four corner-cut tetrahedra and is occupied by $\text{Na}(\text{H}_2\text{O})_4^+$ (orange). The atoms located on the corners of the four small triangles extending out of the void are 12 OH ligands (O3) that come from four $\epsilon\text{-K-Al}_{13}$ groups, indicating that each $\text{Na}(\text{H}_2\text{O})_4^+$ is connected to four $\epsilon\text{-K-Al}_{13}$ groups. (B) The large void is constructed from four inequilateral hexagons (thick yellow lines) that come from four corner-cut tetrahedra and is occupied by four SO_4^{2-} (yellow tetrahedra) and ten interstitial H_2O molecules (pink tetrahedron and octahedron). (C) The connection relationship between two different adjacent cubic octahedral voids (orange and amaranthine) and the corner-cut tetrahedra (cyan) surrounding them. (D) The connection relationship between a central corner-cut tetrahedron and two kinds of cubic octahedral voids surrounding it.

(2.30 Å), and 12 O7–H7...O9 (2.30 Å) hydrogen bonds. The O acceptors (O9, O7, and O6) provided by the members in a small group formed strong hydrogen bonds with the O–H donors (O4–H4 provided by H_2O ligands, and O3–H3 and O2–H2 provided by OH ligands) on the surfaces of the four hexameric rings composed of four $\epsilon\text{-K-Al}_{13}$ groups. Each of the four hexameric rings faced one O6 (H_2O) atom, three O7 (H_2O) atoms, and three SO_4^{2-} ions, forming six O4–H4...O9 (1.85 Å), three O3–H3...O7 (1.97 Å), and three O2–H2...O6 (2.11 Å) hydrogen bonds. In total, the members in each small group contacted with four $\epsilon\text{-K-Al}_{13}$ groups by forming forty-eight strong hydrogen bonds. The strongest (shortest) half of these bonds formed between O4–H4 donors of $\epsilon\text{-K-Al}_{13}$ groups and O9 acceptors of SO_4^{2-} , indicating that strong interactions existed between the polycations and counter-

anions. The connection relation between each $\text{Na}(\text{H}_2\text{O})_4^+$ and four $\varepsilon\text{-K-Al}_{13}$ groups was almost fully controlled by the 12 Na-O3 bonds (2.50 Å when O5 was ordered and 2.54 Å when O5 was disordered, see Table S10). The 12 $\text{O5-H5}\cdots\text{O4}$ hydrogen bonds (2.58 Å) were very weak when the O5 was ordered; even when the O5 atoms were disordered, the 12 $\text{O5A-H5}\cdots\text{O4}$ hydrogen bonds (2.32 Å) were still weak. The Na-O3 bonds and $\text{H5}\cdots\text{O4}$ hydrogen bonds look a little long. Why could they not be further shortened by having the four $\varepsilon\text{-K-Al}_{13}$ groups move closer to the $\text{Na}(\text{H}_2\text{O})_4^+$ in the small void (see Figure 5C)? If this could be done, the hydrogen bonds between the 4S10W unit in the adjacent large void and the four $\varepsilon\text{-K-Al}_{13}$ groups (two of them are shared with the $\text{Na}(\text{H}_2\text{O})_4^+$) surrounding it would be strengthened. However, this did not happen because the distances from the center of a small or large void to the centers (Al1) of the four $\varepsilon\text{-K-Al}_{13}$ groups surrounding it must be $\sqrt{3}a/4$. That is, shortening these distances would decrease the unit cell parameter a . However, the unit cell parameters are almost the same in not only absolute structures A and B but also in reported literature. This indicates that the average Na-O bond length (2.26–2.29 Å) is already optimal for forming the strongest chemical bonds. In other words, the distances between $\varepsilon\text{-K-Al}_{13}$ groups are locked by connection with $\text{Na}(\text{H}_2\text{O})_4^+$, the 3D framework structure of the infinite $\text{Na-}\varepsilon\text{-K-Al}_{13}$ species is rigid, and the SO_4^{2-} and H_2O molecules only passively fill the interstitial voids.

Which absolute structure a crystal belongs to depends on the spatial orientation of the structural motif with respect to the crystal axes. This is because the connection relationships between the corner-cut tetrahedra (each is occupied by an $\varepsilon\text{-K-Al}_{13}$ group), the small corner-cut cubes (each is occupied by $\text{Na}(\text{H}_2\text{O})_4^+$), and the large corner-cut cubes (each is occupied by 4S10W) are the same, as shown in Figure 5CD. For a corner-cut tetrahedron, the four equilateral triangles are equivalent in symmetry, and the four inequilateral hexagons are also equivalent in symmetry, so its spatial orientations are limited in two directions only. If one orientation in which the normal vector of one of the four triangular planes of a corner-cut tetrahedron located on the origin of the unit cell coinciding to the $a + b + c$ vector ([111] direction) is defined as the indicator of absolute structure A, the four corner-cut tetrahedral $\varepsilon\text{-K-Al}_{13}$ groups will certainly keep this orientation with their centers located on the Wyckoff $4a$ sites like the four S atoms in cubic ZnS. Correspondingly, the centers of the four $\text{Na}(\text{H}_2\text{O})_4^+$ will inevitably be located on the $4c$ sites like the four Zn atoms in cubic ZnS, and the centers of the four small groups (each includes 4S10W) will inevitably be located on the $4d$ sites (which are not occupied by any atom in cubic ZnS), as shown in Figure 4AB. Then, relative to the orientation and distribution features in absolute structure A, the other orientation in which the normal vector of one of the four hexagonal planes of a corner-cut tetrahedron located on the origin of the unit cell coinciding to the $a + b + c$ vector is inevitably defined as the indicator of absolute structure B. The four corner-cut tetrahedral $\varepsilon\text{-K-Al}_{13}$ groups will keep this orientation and be located on the Wyckoff $4a$ sites. Correspondingly, the centers of the four small groups will inevitably be located on the $4c$ sites, and the four $\text{Na}(\text{H}_2\text{O})_4^+$ will be positioned on the $4d$ sites, as shown in Figure 4CD. That is, the orientations of the infinite $\text{Na-}\varepsilon\text{-K-Al}_{13}$ species and the distributions of SO_4^{2-} and the interstitial H_2O molecules in absolute structures A and B are different.

Absolute structure A is the inversion result of absolute structure B and *vice versa* (but they are not chiral molecules), as determined by the symmetry of the noncentrosymmetric but achiral $F\bar{4}3m$ space group. Absolute structures A and B are consequently mirror images of each other relative to the xy , yz , and xz planes (but they are not enantiomers of each other), as shown in Figures 2–4, Tables S6–S9 and S6'–S9', and Figures S10–S13 and S10'–S13'.

The discoveries that $\text{Na}_2\text{O}\cdot 13\text{Al}_2\text{O}_3\cdot 8\text{SO}_3\cdot 76\text{H}_2\text{O}$ crystallizes as absolute structure A and B in a 1:1 ratio, the polycations existing in them are all infinite $\text{Na-}\varepsilon\text{-K-Al}_{13}$, $[\text{Na}(\text{H}_2\text{O})_4\text{AlO}_4\text{Al}_{12}(\text{OH})_{24}(\text{H}_2\text{O})_{12}]^{8+}$, and they remain ordered or not depending on the size of the cation coexisting in the mother solution brings us much new knowledge.

First, by adding A_2SO_4 ($\text{A} = \text{Li, Na, K, Rb, or Cs}$) into NaOH -hydrolyzed AlCl_3 solution, colorless T_d single crystals were obtained in each case that had the same unit cell parameter, belonged to the same $F\bar{4}3m$ space group, and had the same structural formula $[\text{Na}(\text{H}_2\text{O})_4\text{AlO}_4\text{Al}_{12}(\text{OH})_{24}(\text{H}_2\text{O})_{12}](\text{SO}_4)_4\cdot 10\text{H}_2\text{O}$. However, these crystals had inverse spatial orientation and distribution, giving two different absolute structures. The statistical results from the analysis of 36 single crystals showed that the A and B conformations formed with equal probability. However, if the atom coordinates of absolute structures A and B were exchanged, their Flack factors would all increase to 0.9 or more, indicating that one is the inversion structure of the other (i.e., A and B are not the same structure). Comparison of our results with relevant literature revealed that the absolute structure A has never been reported. Instead, reported structures^{14,16,50,58} are all absolute structure B and have defects of one kind or another, as listed in Table S11. Also, it has never been reported that the 16 O atoms (labeled as O5 in the asymmetric unit; these atoms are located at the 16e Wyckoff positions, which means that there are 16 symmetrically related O5 atoms in a unit cell) in the four $\text{Na}(\text{H}_2\text{O})_4^+$ in a unit cell (these four $\text{Na}(\text{H}_2\text{O})_4^+$ tightly connect with four $\varepsilon\text{-K-Al}_{13}$ groups to form four $\text{Na-}\varepsilon\text{-K-Al}_{13}$ species; here they were regarded as discrete ions to illustrate the number of coordinated H_2O molecules per Na^+) are ordered. These 16 sites are fully occupied in the crystals obtained by adding Cs_2SO_4 to a NaOH -hydrolyzed AlCl_3 solution. This point is very important for unambiguously determining that the total number of coordinated H_2O molecules in the four $\text{Na}(\text{H}_2\text{O})_4^+$ species is 16. Even if the 16 O5 atoms are disordered as 16 O5A (located at the original 16e Wyckoff positions) and 48 O5B (located at the 48h Wyckoff positions), the sum of their site occupancies should be 16. Therefore, in a construction unit of $\text{Na-}\varepsilon\text{-K-Al}_{13}$, each $\text{Na}(\text{H}_2\text{O})_4^+$ must include four H_2O molecules, regardless of whether they are disordered or not. From the refinement results of the site occupancies of O5A and O5B shown in Figure S3, it was found that from Li^+ to Cs^+ , with an increasing radius of the cations coexisting in the mother solution, the site occupancies of the O5A atoms in the crystallized products continuously rose. The larger the coexisting cation volume, the smaller its thermal ellipsoid. In other words, large coexisting cations restrained the disorder of the four H_2O molecules in $\text{Na}(\text{H}_2\text{O})_4^+$. When the largest cations coexisted in the mother solution (Cs^+), the O5 atoms in the crystallized product become ordered.

Second, our findings clarify some unclear points in the previous literature. The results of structure analysis, XRD, IR, TG, XRF, and density measurements confirmed that the

crystals consist of infinite Na- ϵ -K-Al₁₃ polycations instead of discrete ϵ -K-Al₁₃ ones. The ϵ -K-Al₁₃ groups are connected together with Na(H₂O)₄⁺ by rigid chemical bonds instead of being held together by flexible hydrogen bonds. The number of H₂O molecules coordinated to each Na⁺ is four instead of three and zero, as reported previously. The number of interstitial H₂O molecules in a molecule is ten instead of 11, 12.5, and 20 as reported previously. In addition, the general structural formula is [Na(H₂O)₄MO₄Al₁₂(OH)₂₄(H₂O)₁₂]- (XO₄)₄·10H₂O (M = Al, Ga; X = S, Se) instead of [Na(H₂O)₃AlO₄Al₁₂(OH)₂₄(H₂O)₁₂](SO₄)₄·11H₂O,⁵⁰ Na-[AlO₄Al₁₂(OH)₂₄(H₂O)₁₂](SeO₄)₄·12.5H₂O,¹⁴ Na-[MO₄Al₁₂(OH)₂₄(H₂O)₁₂](SO₄)₄·10H₂O (M = Al, Ga),¹⁶ and Na[GaO₄Al₁₂(OH)₂₄(H₂O)₁₂](SO₄)₄·xH₂O (x ~ 20).⁵⁸

Third, objective positions of all hydrogen atoms were obtained from high-quality single-crystal XRD data, which have either not been given or only a few coordinates of H atoms have been given in previous reports. Knowing the position of hydrogen atoms enabled us to accurately analyze the strength and distribution of hydrogen bonds and to understand the interaction between the infinite polycation and counteranions.

Finally, a formation and evolution mechanism of the infinite Na- ϵ -K-Al₁₃ species was proposed based on its structural features and synthesis conditions. The formation process is illustrated in the TOC graphic, which shows why Na⁺ statistically occupies the four sites (SO = 1/4) that are on the outsides of the four triangular planes of the tetrahedron composed of the four coordinated H₂O molecules of Na(H₂O)₄⁺. This process can be understood as follows: Na⁺ in aqueous solution always exists in the form of hydrated Na(H₂O)_n⁺ (n = 1–5).⁵⁹ When a tetrahedral Na(H₂O)₄⁺ appears in the center of a tetrahedral void surrounded by four triangular planes provided by four corner-cut tetrahedral ϵ -K-Al₁₃ groups, the central Na⁺ could not directly form coordination bonds with the four ϵ -K-Al₁₃ groups because it is already coordinated to four H₂O molecules that would hinder further coordination. Even if the four coordinated H₂O molecules were removed, the Na...O₃ distances (4.2 Å) would be too long to fit the needs of the new coordination environment with 12 OH ligands (O3) in the four directions of a tetrahedron. If Na⁺ shifts out of the coordinated tetrahedron and statistically locates on the outside of its four triangular planes, the tetrahedron will shrink, as shown in Figure 6. In turn, our results indicate that Na(H₂O)₄⁺ probably exists as a tetrahedron rather than a square in aqueous solution, although the latter was observed on the surface of NaCl crystals by Peng and colleagues.⁵⁹ The evolution process from infinite Na- ϵ -K-Al₁₃ to discrete Na- δ -K-Al₁₃ species is

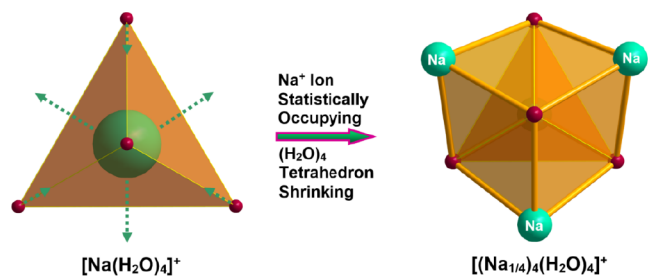


Figure 6. Transformation process from [Na(H₂O)₄]⁺ to [(Na_{1/4})₄(H₂O)₄]⁺, in which one Na⁺ statistically occupies four sites located in a tetrahedral coordination environment.

shown in Figure 7. The chemical equation for this transformation can be written as

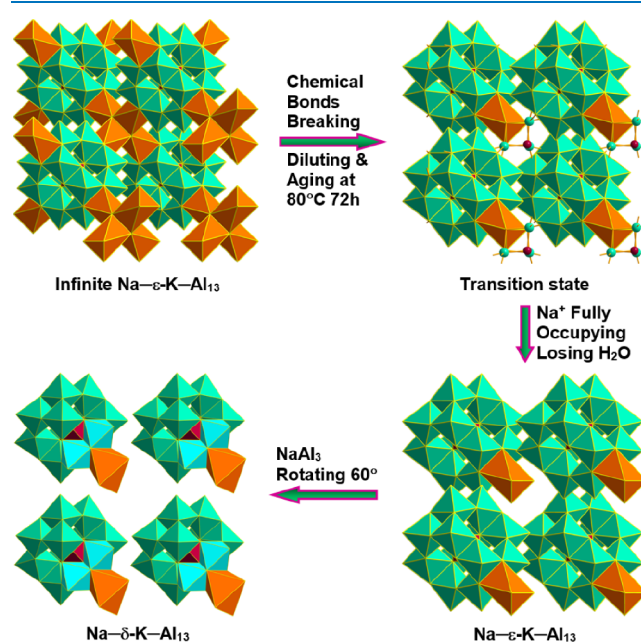
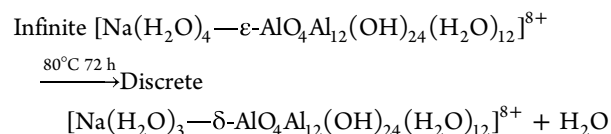


Figure 7. Evolution mechanism from infinite Na- ϵ -K-Al₁₃ ([NaAl₁₃O₄(OH)₂₄(H₂O)₁₆]⁸⁺) to discrete Na- δ -K-Al₁₃ ([NaAl₁₃O₄(OH)₂₄(H₂O)₁₅]⁸⁺) species. NaAl₃ is the [NaAl₃O(OH)₉(H₂O)₆][−] unit composed of one orange NaO₆ octahedron connected to three cyan AlO₆ octahedra.

Therefore, the infinite Na- ϵ -K-Al₁₃ species should be the immediate precursor of the discrete Na- δ -K-Al₁₃ species.

4. CONCLUSION

When A₂SO₄ (A = Li, Na, K, Rb, or Cs) was added to a NaOH-hydrolyzed AlCl₃ solution, a pair of infinite Na- ϵ -K-Al₁₃ species existing in Na₂O·13Al₂O₃·8SO₃·76H₂O were observed. These species have same composition but possess two different absolute structures that are inversion structures and mirror images of each other. The crystallization probabilities of absolute structures A and B are the same. The ionic and crystal structures of the materials were described and their structural features were discussed. Large cations coexisting in the mother solution limited the disorder of the four H₂O molecules in [(Na_{1/4})₄(H₂O)₄]⁺. A formation and evolution mechanism from Na(H₂O)₄⁺ and ϵ -K-Al₁₃ to infinite Na- ϵ -K-Al₁₃ and discrete Na- δ -K-Al₁₃ was proposed. The reasons why infinite Na- ϵ -K-Al₁₃ has a rigid framework structure and one Na⁺ must statistically occupy the four sites in the specific coordination environment were explained. Our findings clarified understanding of ϵ -K-Al₁₃ (or ϵ -K-GaAl₁₂) as a discrete group, and some incorrect structural information in relevant literature was pointed out. These results deepen our understanding of the formation and evolution process of polyaluminum species. As such, they will aid research fields closely related to the hydrolytic

chemistry of aluminum salt solutions, such as geochemistry, environmental science, biochemistry, medicine, and water pollution control chemistry.

■ ASSOCIATED CONTENT

SI Supporting Information

The Supporting Information is available free of charge at <https://pubs.acs.org/doi/10.1021/acsomega.4c00449>.

Information about structurally known polyaluminum species and their classification (Figure S1); corner-cut tetrahedron representation of ε -K-Al₁₃ and the interrelation between the four SO₄²⁻ and ten interstitial H₂O molecules, the connection relationship between Na(H₂O)₄⁺ and ε -K-Al₁₃ groups in infinite Na- ε -K-Al₁₃ species and their spatial orientations, rigid framework structures of infinite Na- ε -K-Al₁₃ species when OS atoms disordered in absolute structure A and B (Figure S2); variation of the thermal ellipsoid size of O5A and O5B statistical atoms in the five products crystallized from mother solutions containing Li⁺, Na⁺, K⁺, Rb⁺, and Cs⁺ (Figure S3); distributions and lengths of hydrogen bonds (Figure S4, Table S1 and S1'); XRD patterns (Figure S5), TG analysis results (Figure S6); measured densities (Table S2); statistical results for absolute structures A and B (Table S3); chemical composition data (Figure S7 and S8, Table S4); IR spectrum (Figure S9, Table S5); structural parameters and inversion relationship of absolute structures A and B (Table S6 and S6', Figure S10 and S10'); structural parameters and mirror-image relationships (Table S7-S9 and S7'-S9', Figure S11-S13 and S11'-S13'); bond lengths and bond angles (Table S10); correspondence of structural parameters (Table S11) (PDF)

Crystallographic data in CIF format for absolute structure A and B. The CIFs may also be obtained from Fachinformationszentrum Karlsruhe 76 344 Eggenstein-Leopoldshafen, Germany [fax (+49)7247-808-666; e-mail crysdata@fiz-karlsruhe.de, website http://www.fiz-karlsruhe.de/request_for_deposited_data.html] upon quoting the depository numbers CSD 2290609-2290612 (CIF, CIF)

■ AUTHOR INFORMATION

Corresponding Author

Zhong Sun – College of Chemistry and Chemical Engineering, Inner Mongolia University, Hohhot 010020, China;
✉ orcid.org/0009-0001-5945-2576; Email: zhong_sun@imu.edu.cn

Authors

Hui Wang – College of Chemistry and Chemical Engineering, Inner Mongolia University, Hohhot 010020, China

Jin-Liang Gu – College of Chemistry and Chemical Engineering, Inner Mongolia University, Hohhot 010020, China

Yu-Wei Guo – College of Chemistry and Chemical Engineering, Inner Mongolia University, Hohhot 010020, China

Yu Ma – College of Chemistry and Chemical Engineering, Inner Mongolia University, Hohhot 010020, China

Ning-Ning Yu – College of Chemistry and Chemical Engineering, Inner Mongolia University, Hohhot 010020, China

Complete contact information is available at: <https://pubs.acs.org/10.1021/acsomega.4c00449>

Author Contributions

All authors contributed equally.

Notes

The authors declare no competing financial interest.

■ ACKNOWLEDGMENTS

We are thankful for the support from the National Natural Science Foundation Committee of China [NNSFC grant 22061030 and 21577072 (to Sun, Z.) and 51468046 (to Wang, H.)].

■ ABBREVIATIONS

ccp, cubic closest packing; SO, site occupancy; 4S10W, four sulfate ions and ten water molecules

■ REFERENCES

- (1) Casey, W. H. Large aqueous aluminum hydroxide molecules. *Chem. Rev.* **2006**, *106*, 1–16.
- (2) Tang, H. X. *Inorganic Polymer Flocculation Theory and Flocculants*; China Architecture & Building Press: Beijing, China, 2006.
- (3) Casey, W. H.; Phillips, B. L.; Furrer, G. Aqueous aluminum polynuclear complexes and nanoclusters: A review. *Rev. Mineral Geochem.* **2001**, *44*, 167–190.
- (4) Bi, S. P.; Wang, C. Y.; Cao, Q.; Zhang, C. H. Studies on the mechanism of hydrolysis and polymerization of aluminum salts in aqueous solution: correlations between the “Core-links” model and “Cage-like” Keggin-Al₁₃ model. *Coord. Chem. Rev.* **2004**, *248*, 441–455.
- (5) Smith, R. W. Reactions among equilibrium and nonequilibrium aqueous species of aluminum hydroxyl complexes. *Adv. Chem. Ser.* **1971**, *106*, 250–256.
- (6) Allouche, L.; Huguenard, C.; Taulelle, F. 3QMAS of three aluminum polycations: Space group consistency between NMR and XRD. *J. Phys. Chem. Solids* **2001**, *62*, 1525–1531.
- (7) Phillips, B. L.; Ohlin, C. A.; Vaughn, J.; Woerner, W.; Smart, S.; Subramanyam, R.; Pan, L. Solid-state ²⁷Al NMR spectroscopy of the γ -Al₁₃ Keggin containing Al coordinated by a terminal hydroxyl ligand. *Inorg. Chem.* **2016**, *55*, 12270–12280.
- (8) Sarpola, A. The hydrolysis of aluminium, a mass spectrometric study. *University of Oulu* **2007**, 279, 1–104.
- (9) Zhao, H.; Liu, H. J.; Qu, J. H. Effect of pH on the aluminum salts hydrolysis during coagulation process: Formation and decomposition of polymeric aluminum species. *J. Colloid Interface Sci.* **2009**, *330*, 105–112.
- (10) Brosset, C.; Biedermann, G.; Sillén, L. G. Studies on the Hydrolysis of Metal Ions. XI. The Aluminium Ion, Al³⁺. *Acta Chem. Scand.* **1954**, *8*, 1917–1926.
- (11) Kohlschütter, H. W.; Hantelmann, P.; Diener, K.; Schilling, H. Basische Aluminiumchloride. *Z. Anorg. Allg. Chem.* **1941**, *248*, 319–344.
- (12) Johansson, G.; Lundgren, G.; Sillén, L. G.; Söderquist, R. On the crystal structure of a basic aluminium sulfate and the corresponding selenate. *Acta Chem. Scand.* **1960**, *14*, 769–771.
- (13) Johansson, G.; Gullman, L.-O.; Kjekshus, A.; Söderquist, R. On the crystal structures of some basic aluminum salts. *Acta Chem. Scand.* **1960**, *14*, 771–773.
- (14) Johansson, G. The crystal structure of a basic aluminum selenate. *Ark. Kemi.* **1963**, *20*, 305–319.

- (15) Johansson, G. On the crystal structure of the basic aluminum sulfate $13\text{Al}_2\text{O}_3 \cdot 6\text{SO}_3 \cdot x\text{H}_2\text{O}$. *Ark. Kemi.* **1963**, *20*, 321–342.
- (16) Parker, W. O., Jr; Millini, R.; Kiricsi, I. Metal substitution in Keggin-type tridecameric aluminum-oxo-hydroxy clusters. *Inorg. Chem.* **1997**, *36*, 571–575.
- (17) Sun, Z.; Wang, H.; Tong, H. G. E.; Sun, S. F. A giant polyaluminum species S-Al_{32} and two aluminum polyoxocations involving coordination by sulfate ions S-Al_{32} and S-K-Al_{13} . *Inorg. Chem.* **2011**, *50*, 559–564.
- (18) Rowsell, J.; Nazar, L. F. Speciation and thermal transformation in alumina sols: Structures of the polyhydroxyoxoaluminum cluster $[\text{Al}_{30}\text{O}_8(\text{OH})_{56}(\text{H}_2\text{O})_{26}]^{18+}$ and its δ -Keggin moiety. *J. Am. Chem. Soc.* **2000**, *122*, 3777–3778.
- (19) Abeysinghe, S.; Unruh, D. K.; Forbes, T. Z. Crystallization of Keggin-type polyaluminum species by supramolecular interactions with disulfonate anions. *Cryst. Growth Des.* **2012**, *12*, 2044–2051.
- (20) Smart, S. E.; Vaughn, J.; Pappas, I.; Pan, L. Controlled step-wise isomerization of the Keggin-type Al_{13} and determination of the γ - Al_{13} structure. *Chem. Commun.* **2013**, *49*, 11352–11354.
- (21) Allouche, L.; Gérardin, C.; Loiseau, T.; Férey, G.; Taulelle, F. Al_{30} : A giant aluminum polycation. *Angew. Chem., Int. Ed.* **2000**, *39*, 511–514.
- (22) Seichter, W.; Mögel, H.; Brand, P.; Salah, D. Crystal structure and formation of the aluminium hydroxide chloride $[\text{Al}_{13}(\text{OH})_{24}(\text{H}_2\text{O})_{24}]\text{Cl}_{15} \cdot 13\text{H}_2\text{O}$. *Eur. J. Inorg. Chem.* **1998**, *1998*, 795–797.
- (23) Sun, Z.; Zhao, H. D.; Tong, H. G. E.; Wang, R. F.; Zhu, F. Z. Formation and structure of $[\text{Al}_{13}(\mu_3\text{-OH})_6(\mu_2\text{-OH})_6(\mu_2\text{-OH})_{12}(\text{H}_2\text{O})_{24}]\text{Cl}_{15} \cdot 13\text{H}_2\text{O}$. *Chin. J. Struct. Chem.* **2006**, *25*, 1217–1227.
- (24) Gatlin, J. T.; Mensinger, Z. L.; Zakharov, L. N.; MacInnes, D.; Johnson, D. W. Facile synthesis of the tridecameric Al_{13} nanocluster $[\text{Al}_{13}(\mu_3\text{-OH})_6(\mu_2\text{-OH})_{18}(\text{H}_2\text{O})_{24}(\text{NO}_3)_{15}]$. *Inorg. Chem.* **2008**, *47*, 1267–1269.
- (25) Wang, W.; Wentz, K. M.; Hayes, S. E.; Johnson, D. W.; Keszler, D. A. Synthesis of the hydroxide cluster $[\text{Al}_{13}(\mu_3\text{-OH})_6(\mu_2\text{-OH})_{18}(\text{H}_2\text{O})_{24}]^{15+}$ from an aqueous solution. *Inorg. Chem.* **2011**, *50*, 4683–4685.
- (26) Casey, W. H.; Olmstead, M. M.; Phillips, B. L. A new aluminum hydroxide octamer $[\text{Al}_8(\text{OH})_{14}(\text{H}_2\text{O})_{18}](\text{SO}_4)_5 \cdot 16\text{H}_2\text{O}$. *Inorg. Chem.* **2005**, *44*, 4888–4890.
- (27) Perkins, C. K.; Eitheim, E. S.; Fulton, B. L.; Fullmer, L. B.; Colla, C. A.; Park, D.-H.; Oliveri, A. F.; Hutchison, J. E.; Nyman, M.; Casey, W. H.; Forbes, T. Z.; Johnson, D. W.; Keszler, D. A. Synthesis of an aluminum hydroxide octamer through a simple dissolution method. *Angew. Chem., Int. Ed.* **2017**, *56*, 10161–10164.
- (28) Hendricks, S. B. The crystal structures of alunite and the jarosites. *Am. Mineral.* **1937**, *22*, 773–784.
- (29) Wang, R.; Bradley, W. F.; Steinfink, H. The crystal structure of alunite. *Acta Crystallogr.* **1965**, *18*, 249–252.
- (30) Menchetti, S.; Sabelli, C. Crystal chemistry of the alunite series: Crystal structure refinement of alunite and synthetic jarosite. In *Neues Jahrb. Mineral., Monatsh.*; Pascal and Francis Bibliographic Databases, 1976; pp 406–417.
- (31) Pabst, A. Some computations on svanbergite, woodhouseite and alunite. *Am. Mineral.* **1947**, *32*, 16–30.
- (32) Tang, Y. Q.; Zhou, G. D.; Hao, R. R. An investigation of crystalline phases in Chinese alunite rocks. *Acta Chim. Sin.* **1957**, *23*, 40–51.
- (33) Okada, K.; Hirabayashi, J.; Osaka, J. Crystal structure of natroalunite and crystal chemistry of the alunite group. In *Neues Jahrb. Mineral., Monatsh.*; Pascal and Francis Bibliographic Databases; 1982; pp 534–540.
- (34) Osaka, J.; Hirabayashi, J.-I.; Okada, K.; Kobayashi, R. Crystal structure of minamiite, a new mineral of the alunite group. *Am. Mineral.* **1982**, *67*, 114–119.
- (35) Altaner, S.; Fitzpatrick, J. J.; Krohn, M. D.; Bethke, P. M.; Hayba, D. O.; Goss, J. A.; Brown, Z. A. Ammonium in alunites. *Am. Mineral.* **1988**, *73*, 145–152.
- (36) Sun, Z.; Wang, H.; Feng, H. J.; Zhang, Y.; Du, S. Y. Crystal structure of $[\text{Al}_4(\text{OH})_6(\text{H}_2\text{O})_{12}][\text{Al}(\text{H}_2\text{O})_6]_2\text{Br}_{12}$: A new polyaluminum compound. *Inorg. Chem.* **2011**, *50*, 9238–9242.
- (37) Johansson, G.; Dorm, E.; Seleborg, M.; Motzfeldt, K.; Theander, O.; Flood, H. The Crystal Structures of $[\text{Al}_2(\text{OH})_2(\text{H}_2\text{O})_8](\text{SO}_4)_2 \cdot 2\text{H}_2\text{O}$ and $[\text{Al}_2(\text{OH})_2(\text{H}_2\text{O})_8](\text{SeO}_4)_2 \cdot 2\text{H}_2\text{O}$. *Acta Chem. Scand.* **1962**, *16*, 403–420.
- (38) Sun, Z.; Wang, H.; Zhang, Y.; Li, J. S.; Zhao, Y.; Jiang, W. N.; Wang, L. One-dimensional infinite chain structures of $[\text{Al}_2(\text{OH})_4(\text{H}_2\text{O})_4]_X$ ($X = \text{I}, \text{Br}, \text{Cl}$): An aggregate of Al_2 species and a precursor of $\text{Al}(\text{OH})_3$. *Dalton Trans.* **2013**, *42*, 12956–12964.
- (39) Sabelli, C.; Ferroni, R. T. The crystal structure of alunite. *Acta Crystallogr.* **1978**, *B34*, 2407–2412.
- (40) Farkas, L.; Pertlik, F. Crystal structure determinations of felsobanyaite and basalunite, $\text{Al}_4[\text{SO}_4][\text{OH}]_{10}[\text{H}_2\text{O}]_4$. *Acta Mineral.-Petrogr.* **1997**, *38*, 5–15.
- (41) Mensinger, Z. L.; Wang, W.; Keszler, D. A.; Johnson, D. W. Oligomeric group 13 hydroxide compounds—a rare but varied class of molecules. *Chem. Soc. Rev.* **2012**, *41*, 1019–1030.
- (42) Bertsch, P. M.; Parker, D. R. *Aqueous Polynuclear Aluminum Species: The Environmental Chemistry of Aluminum*, 2nd ed.; CRC Press: Boca Raton, FL, 1996.
- (43) Jolivet, J. P.; Henry, M.; Livage, J. *Metal Oxide Chemistry and Synthesis: From Solution to Solid State*; John Wiley & Sons: Chichester, U.K., 2000.
- (44) Swaddle, T. W.; Rosenqvist, J.; Yu, P.; Bylaska, E.; Phillips, B. L.; Casey, W. H. Kinetic evidence for five-coordination in $\text{AlOH}(\text{aq})^{2+}$ ion. *Science* **2005**, *308*, 1450–1453.
- (45) Furrer, G.; Phillips, B. L.; Ulrich, K. U.; Pothig, R.; Casey, W. H. The origin of aluminum flocs in polluted streams. *Science* **2002**, *297*, 2245–2247.
- (46) Phillips, B. L.; Casey, W. H.; Karlsson, M. Bonding and reactivity at oxide mineral surfaces from model aqueous complexes. *Nature* **2000**, *404*, 379–382.
- (47) Rustad, J. R.; Loring, J. S.; Casey, W. H. Oxygen-exchange pathways in aluminum polyoxocations. *Geochim. Cosmochim. Acta* **2004**, *68*, 3011–3017.
- (48) Hunter, D.; Ross, D. S. Evidence for a phytotoxic hydroxy-aluminum polymer in organic soil horizons. *Science* **1991**, *251*, 1056–1058.
- (49) Pinnavaia, T. J. Intercalated clay catalysts. *Science* **1983**, *220*, 365–371.
- (50) An, G. Y.; Jiang, Y. Q.; Xi, J. Y.; Liu, L. B.; Wang, P.; Xiao, F.; Wang, D. S. Crystallization of aluminum polycation sulfates: transformation of tetrahedral crystals into block crystals in aqueous solutions. *CrystEngComm* **2019**, *21*, 202–206.
- (51) Sheldrick, G. M. *SADABS: Siemens Area Detector Absorption Correction*; University of Göttingen: Göttingen, Germany, 2008.
- (52) Sheldrick, G. M. *SHELXTL: Bruker Analytical X-ray Systems*; Inc.: Madison, WI, 2008.
- (53) Sheldrick, G. M. SHELXT: Integrating space group determination and structure solution. *Acta Crystallogr., Sect. A: Found. Adv.* **2014**, *70*, C1437–C1437.
- (54) Sheldrick, G. M. SHELXT – Integrated space-group and crystal-structure determination. *Acta Crystallogr., Sect. C: Struct. Chem.* **2008**, *71*, 3–8.
- (55) Zhou, G. D.; Duan, L. Y. *Foundation of Structural Chemistry*, 5th ed.; Peking University Press: Beijing, China, 2017.
- (56) Shannon, R. D. Revised effective ionic radii and systematic studies of interatomic distances in halides and chalcogenides. *Acta Crystallogr.* **1976**, *A32*, 751–767.
- (57) Brandenburg GbR, K.; Putz, H. *Diamond: Crystal and Molecular Structure Visualization*; Crystal Impact: Bonn, Germany, <https://www.crystalimpact.de/diamond>.
- (58) Görz, H.; Schönherr, S.; Pertlik, F. Synthesis and properties of heteropolycation compounds, IV [1]. Synthesis and structure of sodium-dodecaaluminogallium-sulfate-icosihydrate, $\text{Na}[\text{GaO}_4\text{Al}_{12}(\text{OH})_{24}(\text{H}_2\text{O})_{12}](\text{SO}_4)_4 \cdot x\text{H}_2\text{O}$ ($x \sim 20$). *Monatsh. Chem.* **1991**, *122*, 759–764.

(59) Peng, J. B.; Cao, D. Y.; He, Z. L.; Guo, J.; Hapala, P.; Ma, R. Z.; Cheng, B. W.; Chen, J.; Xie, W. J.; Li, X. Z.; et al. The effect of hydration number on the interfacial transport of sodium ions. *Nature* **2018**, *557*, 701–705.